R. & M. No. 3540

MINISTRY OF TECHNOLOGY

AERONAUTICAL RESEARCH COUNCIL
REPORTS AND MEMORANDA

Alleviation of Leading-Edge Heating by Conduction and Radiation

By E. C. CAPEY

LONDON: HER MAJESTY'S STATIONERY OFFICE
1968

PRICE 10*s.* 6*d.* NET

Alleviation of Leading-Edge Heating by Conduction and Radiation

By E. C. CAPEY

Reports and Memoranda No. 3540*
October, 1966

Summary.
A theoretical analysis is made of the equilibrium temperature distribution in the vicinity of the leading edge of a wing of a very high speed aircraft. Results are presented for thermally non-conducting leading edges and for leading edges composed of conducting material or containing inserts of high conductivity material to conduct heat downstream where it is lost by radiation. It is found that for aircraft cruising at Mach 5 the conductivity of typical structural material is sufficiently high to keep the leading-edge temperature down to a level not greatly exceeding that of the rest of the wing; for Mach numbers from 7 to 10 an insert of material of higher conductivity may have to be added. In any case the dependence of leading-edge temperature on leading-edge radius, which is important in the absence of conduction, becomes negligible when conductivity is taken into account.

LIST OF CONTENTS

*Replaces R.A.E. Tech. Report No. 66 311—A.R.C. 28 924.

1. *Introduction.*

Collingbourne and Peckham[1] have studied the aerodynamics of the wing of an aircraft that cruises at speeds from Mach 5 to Mach 10. A caret wing shape is considered, with shape and dimensions as shown in Fig. 1. Such a wing shape appears satisfactory aerodynamically. The kinetic heating of aircraft in the range of Mach number considered is severe, because the equilibrium temperatures are high and because the skin rapidly approaches the equilibrium temperature unless thermally protected. The heating of the leading edge is particularly severe, because the heat transfer coefficient is higher than elsewhere, due partly to the greater air pressure and density and partly to the fact that the thermal boundary layer is thinner.

Earlier investigations[2,3] have shown that for the range of Mach number considered an unprotected structure is competitive with a protected structure from a weight point of view and may be feasible if some form of protection is used to alleviate the excessive temperature that would otherwise obtain in the vicinity of the engines, nose and leading edges. The leading-edge problem is considered here.

A simple method of avoiding an excessive temperature at the leading edge is to adopt a rounded leading edge, rather than a sharp one. However the radius required (assuming the material of the leading edge is non-conducting) to reduce the leading-edge equilibrium temperature to the level of that of the rest of the wing (*see* Fig. 7) is excessive from the aerodynamic standpoint.

An alternative method is to use a skin of high thermal conductivity or to fix an insert of high-conductivity material into the leading edge to conduct some of the heat received at the leading edge a short distance downstream where it is lost by radiation. This method is examined here in more detail.

Calculations are made of the variation of steady state skin temperature with distance from the leading edge for a number of values of Mach number, altitude and leading-edge radius,

(i) for a leading edge with no heat conduction along the skin or into internal structure, and

(ii) for a solid leading edge composed of high-conductivity material, as shown in Fig. 2a, or a leading edge with a high-conductivity insert of the same shape, as shown in Fig. 2b.

The results show how far the leading-edge temperature is reduced by conduction in normal structural material (e.g. stainless steel) and how much further it can be reduced by using a high-conductivity material or by fixing an insert of high-conductivity material in a leading edge of normal structural material. The optimum distribution of a given weight of material is considered.

2. *Heat Transfer and Equilibrium Temperatures.*

2.1. *Description of Flight Conditions and Leading-edge Structure.*

The planform and dimensions of the hypothetical aircraft treated by Collingbourne and Peckham[1] are given in Fig. 1. Since only equilibrium temperatures are calculated the type of internal structure is not relevant. The lower face of the wing is all at an angle $(\alpha + 2{\cdot}6°)$ to the airstream, and the upper face at $(2{\cdot}6° - \alpha)$, where α is the angle of attack. Fig. 1 also gives vertical sections of the leading edge parallel to the air stream and perpendicular to the leading edge. To simplify the analysis the angle of attack is taken to be zero; the effect of varying it is discussed in Section 2.4.

The computations cover all combinations of the following Mach numbers and equivalent air speeds:

$$M = 5,\quad 7,\quad 10$$

$$\begin{aligned} \text{E.A.S.} = {} & 160,\quad 240,\quad 320 \quad \text{m/sec} \\ & (525,\quad 787,\quad 1050 \quad \text{ft/sec}) \end{aligned}$$

Collingbourne and Peckham's results[1] suggest that the above values of equivalent air speed cover the practical range.

To calculate the net heat transfer and surface temperatures information is required on the emissivity of the surface and the ambient air temperature, pressure and density, which can be calculated from the Mach number, equivalent air speed and standard atmospheric properties. A high emissivity is desirable and should be obtainable. Most of the computations have been performed for an emissivity of 0·8, but a few have been repeated using lower values of the emissivity. The atmospheric properties are taken from the following formulae quoted by Naysmith and Woodley[5] as applicable between 25 and 50 km (80 000 and 160 000 ft) above sea level:

$$T = 142{\cdot}2 + 2{\cdot}964\, z, \quad °K \tag{1}$$

where z is the altitude in km,

$$p = 2409 \left(\frac{217{\cdot}3}{T}\right)^{11{\cdot}39} \quad N/m^2 \tag{2}$$

and

$$\rho = 3{\cdot}49 \times 10^{-3} \frac{p}{T} \quad kg/m^3 \tag{3}$$

The above formulae give the atmospheric properties as functions of altitude. They may be expressed instead in terms of Mach number and equivalent air speed by making use of the relationships

$$M = \frac{v}{20{\cdot}06\sqrt{T}} \tag{4}$$

and

$$\text{E.A.S.} = v\sqrt{\rho/\rho_0}, \quad \text{m/sec} \tag{5}$$

where v is the velocity in m/sec and ρ_0 the standard air density at sea level, 1·223 kg/m^3. Table 1 lists the atmospheric properties as calculated from equations (1) to (5) for the Mach numbers and equivalent air speeds considered.

2.2. *Heat Transfer to Straight Sections of Wing.*

In this section, which is based largely on a report by Naysmith and Woodley[5], the heat transfer to the straight sections of the wing (PQ and $P'Q'$ in Fig. 1) is examined. As the angle of attack is taken to be zero, the heat transfer and equilibrium temperatures are the same on the two surfaces.

The aerodynamic heat input, expressed in terms of enthalpies per unit mass of air, is

$$q_{\text{aero}} = h_i\,(i_r - i_s), \tag{6}$$

where q_{aero} is the rate of heat input per unit area, h_i a heat-transfer coefficient (based on enthalpy), i_s the enthalpy per unit mass of air at the temperature of the surface and i_r a recovery enthalpy per unit mass. The latter is given by the equation

$$i_r = i_\infty + \tfrac{1}{2} r v^2 , \tag{7}$$

where i_∞ is the enthalpy of the free air, v the velocity, and r a recovery factor, which is about 0·89 for turbulent flow and 0·86 for laminar flow. Table 2 gives the recovery enthalpies for the nine combinations of Mach number and equivalent air speed considered.

The value of the heat-transfer coefficient h_i depends on whether the flow is laminar or turbulent. There is reason to expect[1,6] it to be laminar near the leading edge but to become turbulent downstream. The following formulae for heat-transfer coefficients have been used by several writers (e.g. Naysmith and Woodley[5]).

Laminar flow:

$$h_i = 0{\cdot}332\,(v_1\,\rho^*\,\mu^*/y)^{\frac{1}{2}}\,(Pr^*)^{-2/3} \tag{8}$$

Turbulent flows:

$$h_i = 0{\cdot}144\,S^*\,\rho^*\,v_1\,[\log_{10}(\rho^*\,v_1\,y/\mu^*)]^{-2{\cdot}45} , \tag{9}$$

where v_1 is the velocity of the air relative to the aircraft after passing through the shock wave, i_1 its enthalpy per unit mass and where the starred material properties are the properties of air at the temperature of intermediate enthalpy i^* as defined by the equation

$$i^* = 0{\cdot}22\,i_r + 0{\cdot}28\,i_1 + 0{\cdot}50\,i_s . \tag{10}$$

The constant S^* is the Reynolds' analogy factor, taken to be 1·22. The distance y in equation (9) is the distance from the onset of turbulence; in equation (8) y is the distance from a sharp leading edge. For laminar flow from the rounded leading edge analysed here there is doubt as to the correct origin for y, and an arbitrary constant y_0 is added to y, whose value is determined when the heat inputs on the straight and rounded sections are equated at their junction. The atmospheric properties appearing in equation (8) vary with the temperature of intermediate enthalpy, which depends on the flight conditions and the surface temperature. The variation with surface temperature is slight and is neglected so that equation (8) becomes

$$h_i = \frac{C}{\sqrt{x + x_0}} \tag{11}$$

where C is constant for given flight conditions, x is the normal distance from the leading edge as shown in Fig. 1d, and x_0 replaces y_0.

Equilibrium temperatures are obtained by balancing the aerodynamic heat input q_{aero} (as given by equations (6) to (9) for a sharp leading edge and equation (11) for a founded leading edge) against the radiative output per unit area:

$$q_{rad} = \varepsilon\,\sigma\,T_s^4 , \tag{12}$$

where ε is the emissivity, σ the Stefan-Boltzmann constant and T_s the surface temperature.

Figs. 4 and 5, which are obtained from Naysmith and Woodley's results[5], give equilibrium temperatures on the surface of a sharp wedge of half angle 2·6° Fig. 4 gives equilibrium temperatures under turbulent flow conditions at a distance parallel to the air stream of 15 m (50 ft) from the onset of turbulence. These

temperatures are a measure of the heating of the bulk of the wing surface, and in the present context the problem of leading-edge heating may be taken as solved if the leading-edge temperature is kept down to the level given by Fig. 4. Fig. 5 gives equilibrium temperatures under laminar-flow conditions at 0·915 m (3 ft) from the leading edge measured parallel to the airstream, which corresponds to a distance of 0·237 m ($8\frac{1}{2}$ in.) normal to the leading edge.

Comparison of the equilibrium temperatures at 15 m and 0·915 m from the leading edge shown in Figs. 4 and 5 respectively with the stagnation line equilibrium temperatures, calculated in the next Section and shown in Fig. 7, demonstrates that the excess leading-edge heating is very localised.

2.3. *Heat Transfer to Rounded Leading Edge.*

The heat transfer to the rounded section of the leading edge was calculated by the method of Beckwith and Gallagher[4], in which the heat-transfer coefficient based on enthalpy, h_i, is taken to vary as

$$h_i = C' f(\theta)/\sqrt{R}, \tag{13}$$

where R is the leading edge radius, θ the angular distance from the stagnation line, $f(\theta)$ an empirically determined function shown in Fig. 6, and where C' depends on the Mach number, ambient conditions, angle of attack and surface temperature. The values of C' for the Mach numbers and equivalent air speeds considered were calculated for a skin temperature of 1000°K, and are listed in Table 3, as are the values of C in equation (11) for heat transfer to the straight sections of the skin. The dependence of C' and C on surface temperature is slight, and is neglected.

The heat-transfer rates given by equations (11) and (13) must be equal at the junction of the straight and rounded sections ($\theta = 80°$, $x = 1{\cdot}396\,R$), from which it follows that

$$\frac{C' f(80°)}{\sqrt{R}} = \frac{C}{\sqrt{1{\cdot}396\,R + x_0}}. \tag{14}$$

Putting $f(80°)$ equal to 0·213 (from Fig. 6) and substituting the values of C and C' listed in Table 3, values of x_0/R were calculated from equation (14), and these are also listed in Table 3.

The aerodynamic heat input per unit area along the stagnation line can be calculated, by means of equations (6) and (13), for given values of the leading-edge radius R, the surface temperature T_s and the quantities i_r and C' given in Tables 2 and 3. Balancing this against the radiative heat output, and assuming no heat conduction, the stagnation-line equilibrium temperature, T_{eq}, is given by the equation

$$\frac{C'}{\sqrt{R}}(i_r - i_{eq}) = \varepsilon\,\sigma\,T_{eq}^4. \tag{15}$$

where the enthalpy per unit mass, i_{eq}, is proportional to the temperature, T_{eq}, multiplied by the mean specific heat of air between absolute zero and T_{eq}. In the range of surface temperature of interest the specific heat of air may be taken to be 1·0 $J\ gm^{-1}\ °K^{-1}$, so that in MKS units equation (15) becomes

$$\frac{C'}{\sqrt{R}}(i_r - 1000\,T_{eq}) = \varepsilon\,\sigma\,T_{eq}^4. \tag{16}$$

Fig. 7 shows leading-edge stagnation-line temperatures, calculated from equation (16), plotted against the leading-edge radius R, for an equivalent air speed of 240 m/sec (787 ft/sec) and Mach numbers of 5, 7 and 10. It is seen by comparing Figs. 7 and 4 that, even with a very large radius, the leading-edge equilibrium temperature considerably exceeds that of the rest of the wing.

2.4. *Effect of Angle of Attack.*

To estimate the influence of angle of attack equilibrium temperatures have been evaluated for an equivalent air speed of 240 m/sec, a surface emissivity of 0·8 and a lower-surface pressure coefficient of 0·05, which corresponds under these conditions to an angle of attack of 2·8° at Mach 5, 3·8° at Mach 7 or 4·5° at Mach 10. These results are compared against those obtained for a zero angle of attack.

Columns (5) and (6) in Table 4 show the influence of angle of attack on the turbulent equilibrium temperature on the lower face, which is taken as a measure of the severity of heating of the bulk of the wing. The increase in temperature is considerable, rising from 31° at Mach 5 to 178° at Mach 10.

Columns (7) and (8) show the influence of angle of attack on the laminar heat transfer to the straight section of the wing close to the leading edge. The increase in equilibrium temperature on the lower face is less than for the turbulent case, rising from 18° at Mach 5 to 99° at Mach 10. If, moreover, the upper and lower faces are thermally connected, as they can be close to the leading edge, the true increase in temperature is approximately equal to the mean of the increases in equilibrium temperature of the upper and lower faces, which rises from 1° at Mach 5 to 22° at Mach 10.

Column (9) gives the percentage increases in heat-transfer coefficient on the stagnation line due to angle of attack: this rises from 2 per cent at Mach 5 to 4 per cent at Mach 10. It is seen from the value of C' listed in Table 3 that the heat-transfer coefficient is roughly proportional to the equivalent air speed, so that these increases in heat-transfer coefficient are equivalent to proportionate increases (2 per cent to 4 per cent) in equivalent air speed. Anticipating the results of Section 3, columns (10) and (11) in Table 4 show the influence such changes of equivalent air speed have on the temperature of one of the conducting leading edges analysed in that section.

These results show that the influence of angle of attack on leading-edge heating is slight. The situation is complicated by variation of heat transfer round the cylindrical section of the leading edge and by changes in the constant x_0 in the heat-input equation for the straight sections. These complications should not, however, seriously alter the situation, and it may be taken that the leading-edge temperature for a typical angle of attack only slightly exceeds that for a zero angle of attack, but that the temperature of the lower face of the wing, with which the leading-edge temperature must be compared, increases considerably.

3. *Heating of Leading Edge Composed of Conducting Material.*

3.1. *Analysis.*

Steady state temperatures have been computed for leading edges composed of conducting material with a thickness variation as shown in Fig. 3a. The choice of distribution of conducting material was based on the following considerations:

(i) The variation of thickness should be continuous, since it can be shown that the thermal conductance of a discontinuous section is improved by modifying the shape to a continuous one.

(ii) Ideally the thickness should decrease in a chordwise direction. Conducting material is more valuable close to the leading edge, as the heat flow there is high and as it is the leading-edge temperature which needs to be reduced. However, the shape of the leading edge limits the allowable thickness of conducting material. The leading edge is therefore solid to a point F, beyond which the thickness of conducting material reduces continuously.

(iii) The optimum shape of distribution beyond F is difficult to determine, but an exponential distribution with an arbitrary constant D should give temperatures not greatly in excess of the optimum for a given quantity of conducting material.

In the distribution of material in Fig. 3 there are two arbitrary parameters R' and D (in addition to the leading edge radius R), which may be varied arbitrarily. In the discussion to follow, however, R' and A are treated as the independent variables, where A is the cross-sectional area of conducting material, expressible in terms of R, R' and D as follows:

$$A = 4\pi R^2/9 + (R'^2 - R^2)\cot 10° + 2DR'. \tag{17}$$

The steady state heat conduction equations within the conducting material are solved by a finite difference method, in which the material is divided into 31 segments numbered 2, 4 . . . 62 as shown in Fig. 3b. All segments have unit length in a direction parallel to the leading edge. Variations of temperature normal to the surface are neglected; this step was justified on the basis of a preliminary investigation, as outlined below.

(i) Temperature distributions along the skin were computed neglecting temperature variation normal to the skin.

(ii) The temperature variation normal to the skin was treated as a perturbation on the distribution along the skin, and was calculated from the steady state heat conduction equation

$$\left(\frac{\partial^2}{\partial x^2}+\frac{\partial^2}{\partial z^2}\right) T = 0, \qquad \begin{matrix} x \text{ along skin} \\ z \text{ normal to skin} \end{matrix} \tag{18}$$

using values of the differential $\partial^2 T/\partial x^2$ taken from the unperturbed solution, so that

$$\left(\frac{\partial^2 T}{\partial z^2}\right)_{\text{perturbed}} = -\left(\frac{\partial^2 T}{\partial x^2}\right)_{\text{unperturbed}} \tag{19}$$

This equation was integrated with respect to z to give the difference $(T_s - T_i)$ between the surface temperature and the temperature on the inner face of the conducting material (or on the centreline for sections forward of F).

(iii) Temperature differences $(T_s - T_i)$, evaluated at various points on the skin for several of the cases computed, in no case exceeded 3 deg. The neglect of normal variation of temperature is therefore justified.

The steady-state temperature distribution is obtained by equating to zero the total heat input into each segment, which is composed of aerodynamic, radiative and conductive terms. The aerodynamic heat input for segments in the straight section of the skin ($n = 4$ to 62) is expressed in the following form derived from equations (6) to (11):

$$Q_{\text{aero},n} = \frac{A_n C (i_r - 1000\, T^n)}{\sqrt{x_n + x_0}}, \tag{20}$$

where A_n is the surface area of the nth segment, x_n the distance of the centre of the segment from the stagnation line measured along the surface and T_n its mean temperature. For the rounded segment

$$Q_{\text{aero},2} = \frac{0{\cdot}675\, A_2\, C'}{\sqrt{R}} (i_r - 1000\, T_2). \tag{21}$$

The radiative heat input is

$$Q_{\text{rad},n} = -A_n \varepsilon \sigma T_n^4, \tag{22}$$

and the conductive heat input

$$Q_{\text{cond},n} = K_{n-1}(T_{n-2} - T_n) - K_{n+1}(T_n - T_{n+2}), \tag{23}$$

where the constants K_{n-1}, K_{n+1} are thermal conductances between adjacent segments. If b_{n+1} is the thickness of the conducting material between the nth and $(n+2)$nd segments, k its conductivity and x_n and x_{n+2} the distances of the centres of the segments from the leading edge, the conductance K_{n+1} between these segments is

$$K_{n+1} = \frac{k\, b_{n+1}}{x_{n+2} - x_n}. \tag{24}$$

Conduction downstream from the last segment ($n = 62$) is taken to be zero.

Steady-state temperature distributions are obtained by solving the 31 simultaneous equations obtained by equating to zero the total heat input into each segment, as given by equations (20) to (24). In view of the large number of segments used to represent the straight section of the skin, the finite-difference equations are an accurate representation of the differential equations obeyed by the conducting material. Treating the rounded section as a single segment could introduce appreciable error for large leading-edge radii. For a radius of 2 mm, however, temperature variations within the rounded segment do not exceed 10 to 15 deg even for the Mach 10 case, so the error in the approximation is acceptable.

If the leading-edge heating is not too severe the solid leading edge may be composed of the same material as the rest of the wing. If the heating is more severe a different material of higher conductivity may be required. This may be attached as a solid leading edge or else fixed as an insert in a leading edge composed of the same material as the rest of the wing, as shown in Fig. 2b. The computed temperatures still apply approximately if the conducting material is used as an insert provided there is a good bond between the two materials. The manufacturing problems involved in fixing an insert of material into a leading edge require experimental investigation and are not considered here.

3.2. *Discussion of Results.*

Leading-edge temperatures in conducting leading edges with the configuration of Fig. 3 are given in Table 5 for a number of combinations of the following data:

Mach number	5, 7, 10
Equivalent air speed	160, 240, 320 m/sec (525, 787, 1050 ft/sec)
Leading-edge radius	1, 2, 5 mm (0·04, 0·08, 0·20 in.)
Emissivity	0·4, 0·6, 0·8
Conductivity of conducting material	24, 59, 118 watt m^{-1} °K^{-1}
Cross-sectional area	2·5, 5, 10 cm^2 (0·39, 0·78, 1·55, in^2)
Maximum thickness (R')	Optimised.

The first six variables listed above were treated as independent parameters, and a sufficient number of combinations of the values quoted above were solved to enable one to see the significance of each parameter and to estimate leading-edge temperatures for any other case which falls within the ranges of the parameters listed above.

For each combination of these six variables solutions were computed for a number of values of the maximum thickness R' of conducting material till the minimum leading-edge temperature obtainable by varying R' was obtained. In view of the small changes in leading-edge temperature produced by changes in R' in the vicinity of the optimum, an accurate estimate of the optimum value of R' was not necessary, and as the pattern of results became clear interpolated values of R' were used for some cases. For this reason optimum values of R' are not listed beside the leading-edge temperatures in Table 5, but they are discussed later.

The results in Table 5 show that the leading-edge temperature depends on the Mach number more than on any other variable, the next most significant being the emissivity and the conductivity. High emissivity is desirable and most of the results are computed for an emissivity of 0·8, which it is believed should be obtainable in practice.

The higher conductivity of 118 watt m^{-1} $°K^{-1}$ is typical of some forms of graphite, which are suitable materials for use as inserts because of their high melting point, high conductivity and moderately low density. For temperatures below its melting point (933°K) pure aluminium has thermal properties superior to those of graphite, having a thermal conductivity 60 per cent higher and approximately the same density. Pure magnesium and copper are also competitive. The choice of material may, however, be determined by manufacturing considerations. If graphite is used, and its density is taken to be 2·8 gm/cm^3, the cross-sectional area of 5 cm^2 corresponds to a weight of 1·4 kg per metre of leading edge (0·94 lb/ft).

The lower conductivity of 24 watt m^{-1} $°K^{-1}$ is that of stainless steel at 700°K and is also typical of nimonic alloy and other structural materials suitable for high speed aircraft. The steel leading edge of cross-sectional area 2·5 cm^2 considered weighs 2·1 kg per metre of leading edge, but as it has a structural as well as a thermal function it is comparable from a weight point of view with the 5 cm^2 insert of graphite (weighing 1·4 kg per metre) and is compared with it in Table 5 and Fig. 7. It is seen that the advantage of using a high conductivity material like graphite is small at Mach 5 but increases with Mach number.

Comparison of the results given in Table 5 and Fig. 4 shows that, if the angle of attack is zero, a leading edge with a 5 cm^2 insert of graphite reaches a temperature exceeding that of the lower face of the wing by about 30 deg at Mach 5, 140 deg at Mach 7 and 320 deg at Mach 10. On the other hand the stainless steel leading edge considered above gives temperatures 90 deg, 250 deg and 510 deg in excess of those of the lower face of the wing.

If an angle of attack is chosen sufficient to give a lower surface pressure coefficient of 0·05, then the temperature of the lower face of the wing is considerably increased, as shown in Table 4, while the heat input to the leading edge is only slightly increased, the increase in heat input on the stagnation line being equivalent to an increase in equivalent air speed of 2 per cent at Mach 5, 3 per cent at Mach 7 and 4 per cent at Mach 10. The effect of these increases in equivalent air speed on the temperature of a conducting leading edge of 2 mm radius with a 5 cm^2 insert of graphite is estimated from the results given in Table 5 and shown in the last two columns of Table 4. Comparison with the results for the temperature of the lower face of the wing (Table 4 column (5)) shows that, if the angle of attack is chosen to give a lower surface pressure coefficient of 0·05, then at Mach 5 the leading edge attains the same temperature as the lower face of the wing, at Mach 7 it attains a temperature about 60 deg higher and at Mach 10 about 160 deg higher. The comparable excess temperatures of the stainless steel leading edge are 60 deg, 170 deg and 350 deg.

Comparison of Table 5 and Fig. 7 shows that the leading-edge temperatures attained with a 5 cm^2 insert of graphite are well below those attained by blunting the leading edge, unless the leading-edge radius is increased to about 0·1 metres, which is aerodynamically unacceptable.

The results given in Table 5 show that variations in equivalent air speed, leading-edge radius and area of conducting material all influence the leading-edge temperature considerably less than variations of Mach number. Reduction of the equivalent air speed from 240 m/sec to 160 m/sec reduces the leading-edge temperature by 31 deg at Mach 5 and 103 deg at Mach 10. Halving the quantity of conducting material raises the leading-edge temperature by 15 deg at Mach 5 and 32 deg at Mach 10.

The effect of changes of leading-edge radius is slight; a change from a 2 mm to a 5 mm radius reduces the leading-edge temperature only 4 deg at Mach 5 and 3 deg at Mach 10. There is thus no objection to a sharp leading edge if it is desired on aerodynamic grounds.

The optimum value of R', the maximum thickness of conducting material, was found to be about 5 mm at Mach 5, 6 mm at Mach 7 and 7 mm at Mach 10 for a leading edge with a 2 mm radius and 5 cm^2 of material of conductivity 118 watt m^{-1} $°K^{-1}$. Halving the area of conducting material reduces it by a factor of about $\sqrt{2}$; halving the conductivity increases it by about the same factor, and the equivalent air speed and leading-edge radius have a minor influence.

4. *Conclusions.*

If the leading edge of a typical aircraft cruising between Mach 5 and Mach 10 is not thermally protected and is composed of non-conducting material, it attains a temperature hundreds of degrees in excess of that of the rest of the wing. This problem, while severe for any leading edge, becomes even more severe for the sharp leading edges desired on aerodynamic grounds.

It is shown that the temperature of a leading edge composed of steel or nimonic alloy is considerably reduced by conduction, particularly if it is solid for the first few centimetres, and that it can be further reduced by making the leading edge of high conductivity material or by fixing into it an insert of high conductivity material. At Mach 5 a solid stainless steel leading edge with about 1·4 kg/m (0·94 lb/ft) of additional material added to increase its conductivity attains a steady temperature only about 60 deg higher than that of the rest of the wing. For speeds betweem Mach 7 and Mach 10 the excess leading-edge temperature is considerably greater, but may be reduced to an acceptable level by using a leading edge of high conductivity material or by fixing an insert of high conductivity material into a leading edge composed of the same material as the rest of the wing. It is found that an insert of 1·4 kg/m of graphite reduces the leading-edge temperature to within 60 deg of that of rest of the wing at Mach 7 and 160 deg at Mach 10.

It is found that with conduction present the temperature of the leading edge is almost independent of its radius. The leading edge may therefore be made as sharp as desired.

If special high conductivity material is to be used at the leading edge there are several manufacturing problems requiring experimental investigation. If the high conductivity material is to be used as an insert the main problem is that of fixing the insert into the leading edge in such a manner as to retain good thermal contact even when heating causes differential expansion of the insert and skin materials. If, on the other hand, the high conductivity material is to be used as a complete leading edge, the main problems are rain erosion, atmospheric erosion and corrosion at elevated temperature and fixing of the leading edge to the rest of the wing.

It should be borne in mind that the present investigation is for a fixed wing sweepback angle and that the beneficial effect of conduction would be expected to diminish with reducing sweepback.

Acknowledgment.

The author wishes to thank Mr. A. Naysmith of the Ministry of Technology for his help with this work.

LIST OF SYMBOLS

A	Cross-sectional area of conducting material
A_n	Outwards facing area of nth section
b	Thickness of conducting material
C	Constant in equation (11)
C'	Constant in equation (13)
c_p	Specific heat of air under constant pressure
C_p	Pressure coefficient
D	Constant in distribution of conducting material
$f(\theta)$	Function in equation (13)
$\bar{f}(\theta)$	Mean value of $f(\theta)$
h_i	Heat-transfer coefficient based on enthalpy
i_{eq}	Equilibrium enthalpy per unit mass of air
i_r	Recovery enthalpy per unit mass of air
i_∞	Enthalpy distant from aircraft per unit mass of air
i^*	Intermediate enthalpy given by equation (10)
k	Thermal conductivity
K_{n+1}	Conductance between sections n and $(n+2)$
M	Mach number
p	Pressure
P_r	Prandtl number $= \mu c_p/k$
q_{aero}	Aerodynamic heat input per unit area
q_{rad}	Radiative heat output per unit area
$Q_{\text{aero},n}$	Aerodynamic } heat input to a segment
$Q_{\text{rad},n}$	Radiative } heat input to a segment
$Q_{\text{cond},n}$	Conductive } heat input to a segment
r	Recovery factor
R	Leading-edge radius
R'	Constant in distribution of conducting material
S^*	Reynolds analogy factor
T	Temperature (absolute)
T_{eq}	Equilibrium temperature

v	Velocity
x	Normal distance from leading edge
x_0	Constant in equation (11)
x''	Dimension shown in Fig. 2a
y	Distance parallel to airstream
y_0	Constant to be added to y in equation (8)
z	Altitude Also co-ordinate normal to skin
α	Angle of attack
ε	Emissivity
θ	Angular distance from stagnation line
μ	Viscosity
ρ	Density
ρ_0	Standard sea level air density
σ	Stefan-Boltzmann constant

Subscripts

1	Properties beyond shock wave
i	Inner face of conducting material
n	Number of segment
s	Surface
*	Properties at temperature of intermediate enthalpy

REFERENCES

No.	*Author(s)*	*Title, etc.*
1	J. R. Collingbourne and D.H. Peckham ..	The lift and drag characteristics of caret wings at Mach numbers between 5 and 10. A.R.C. C.P. 930, February 1966.
2	E. C. Capey	Alleviation of thermal stresses in aircraft structures. A.R.C. C.P. 819, November 1964.
3	M. O. W. Wolfe	Aspects of elevated temperature design and design criteria for supersonic aircraft structures. R.A.E. Report Structures 288 (A.R.C. 24 982), May 1963.
4	I. E. Beckwith and J. J. Gallagher	Local heat transfer and recovery temperatures on a yawed cylinder at a Mach number of 4·15 and high Reynolds numbers. NASA TR R–104, 1961.
5	A. Naysmith and J. G. Woodley	Equilibrim temperatures on lifting surfaces at Mach numbers between 5 and 12 at altitudes from 80 000 ft up to 150 000 ft. R.A.E. Technical Report No. 67 114, May 1967.
6	D. R. Topham	A correlation of leading edges transition and heat transfer on swept cylinders in supersonic flow. A.R.C. 26 219, August 1964.

TABLE 1

Flight Conditions and Atmospheric Properties

Mach number	Equivalent air speed m/sec	Pressure N/m^2	Temperature °K	Density gm/m^3	Velocity m/sec	Altitude km
Obtained from equations:		(3), (4) and (5)	(2)	(3)	(4)	(1)
5	160 (525 ft/sec)	891 (18·6 lb/ft^2)	237·1	13·08 (818×10^{-6} lb/ft^3)	1544 (5 060 ft/sec)	32·01 (105 000 ft)
5	240	2005	220·9	31·59	1490	26·55
5	320	3565	209·9	59·11	1453	22·84
7	160	455	251·6	6·293	2227	36·91
7	240	1023	234·3	15·19	2149	31·07
7	320	1819	222·7	28·42	2097	27·16
10	160	223	267·8	2·898	3280	42·37
10	240	501	249·5	6·988	3170	36·20
10	320	891	237·1	13·08	3090	32·01

Sea level air density $\rho_0 = 1223$ gm/m^3 (0·0764 lb/ft^3)

Sea level air pressure $= 1{\cdot}012 \times 10^5$ N/m^2 (2116 lb/ft^2)

TABLE 2

Recovery Enthalpies per Unit Mass of Air

Mach number	Equivalent air speed m/sec	Enthalpy of free air i_∞ J/gm	Enthalpy due to stagnation $\frac{1}{2}v^2$ J/gm	Recovery enthalpy i_r laminar flow J/gm	Recovery enthalpy i_r turbulent flow J/gm
5	160 (525 ft/sec)	237	1192	1262	1298
5	240 (787 ft/sec)	221	1110	1176	1209
5	320 (1050 ft/sec)	210	1056	1118	1150
7	160	252	2480	2385	2459
7	240	234	2309	2220	2289
7	320	223	2199	2114	2180
10	160	268	5379	4894	5055
10	240	250	5024	4571	4720
10	320	237	4774	4343	4486

Recovery temperatures may be calculated from the recovery enthalpies and the specific heat of air. Up to 1000°K the specific heat of air is 1·0 J gm^{-1} $°K^{-1}$, so that 1 J/gm in i_r corresponds to 1 deg K in recovery temperature.

TABLE 3

Constants in Heat Input Equations

Mach number	Equivalent air speed m/sec	C kg sec^{-1} m$^{-1\frac{1}{2}}$	C' kg sec^{-1} m$^{-1\frac{1}{2}}$	$\frac{x_0}{R}$
5	160 (525 ft/sec)	$3{\cdot}723 \times 10^{-3}$	$9{\cdot}68 \times 10^{-3}$	1·87
5	240 (787 ft/sec)	$5{\cdot}401 \times 10^{-3}$	$14{\cdot}39 \times 10^{-3}$	1·72
5	320 (1050 ft/sec)	$6{\cdot}945 \times 10^{-3}$	$18{\cdot}76 \times 10^{-3}$	1·63
7	160	$3{\cdot}145 \times 10^{-3}$	$9{\cdot}70 \times 10^{-3}$	0·93
7	240	$4{\cdot}609 \times 10^{-3}$	$14{\cdot}55 \times 10^{-3}$	0·81
7	320	$5{\cdot}983 \times 10^{-3}$	$19{\cdot}25 \times 10^{-3}$	0·73
10	160	$2{\cdot}644 \times 10^{-3}$	$10{\cdot}14 \times 10^{-3}$	0·10
10	240	$3{\cdot}834 \times 10^{-3}$	$15{\cdot}04 \times 10^{-3}$	0·04
10	320	$5{\cdot}111 \times 10^{-3}$	$19{\cdot}98 \times 10^{-3}$	0·05

TABLE 4

Effect of Angle of Attack.

(1) Mach number	(2)	(3) Inclination to airstream	(4) Pressure coefficient C_p	(5) T_{eq} turbulent flow °K	(6) ΔT_{eq} turbulent flow	(7) T_{eq} laminar flow °K	(8) ΔT_{eq} laminar flow	(9) % increase in heat transfer coefficient	(10) T_{eq} Conducting leading edge °K	(11) ΔT_{eq} Conducting leading edge
5	$\alpha = 0$	2·6°	0·021	738		610			768	
	$C_p = 0{\cdot}05$ upper face	−0·2°				594	−16	2%	769	1
	$C_p = 0{\cdot}05$ lower face	5·4°	0·050	769	31	628	18			
7	$\alpha = 0$	2·6°	0·016	882		745			1019	
	$C_p = 0{\cdot}05$ upper face	−1·2°				715	−30	3%	1024	5
	$C_p = 0{\cdot}05$ lower face	6·4°	0·050	966	84	790	45			
10	$\alpha = 0$	2·6°	0·012	1015		894			1337	
	$C_p = 0{\cdot}05$ upper face	−1·9°				840	−54	4%	1350	13
	$C_p = 0{\cdot}05$ lower face	7·1°	0·050	1193	178	993	99			

Equivalent air speed = 240 m/sec (787 ft/sec)
Emissivity = 0·8
T_{eq} turbulent flow – 15 metres from onset of turbulence (50 ft)
T_{eq} laminar flow – 0·915 metres from sharp leading edge (3 ft)

TABLE 5

Equilibrium Temperatures of Conducting Leading Edges.

Mach number	E.A.S. (m/sec)	Emissivity	Leading edge radius (mm)	Conductivity (watt $m^{-1}\,°K^{-1}$)	Cross-sectional area A (cm^2)	T_{eq} at leading edge (°K)	Property varied
5	160 240 320	0·8	2	118	5	737 768 783	E.A.S.
5	240	0·4 0·6 0·8	2	118	5	851 802 768	Emissivity
5	240	0·8	1 2 5	118	5	772 768 764	Radius
5	240	0·8	2	24 59 118	2·5 5 5	824 788 768	Conductivity
5	240	0·8	2	118	2·5 5 10	783 768 754	Area
7	160 240 320	0·8	2	118	5	954 1019 1062	E.A.S.
7	240	0·4 0·6 0·8	2	118	5	1159 1076 1019	Emissivity

Some results appear in the Table more than once to make comparison easier.

TABLE 5 (*continued*)

Equilibrium Temperatures of Conducting Leading Edges.

Mach number	E.A.S. (m/sec)	Emissivity	Leading edge radius (mm)	Conductivity (watt m^{-1} °K^{-1})	Cross-sectional area A (cm^2)	T_{eq} at leading edge (°K)	Property varied
7	240	0·8	2	24 59 118	2·5 5 5	1128 1058 1019	Conductivity
7	240	0·8	2	118	2·5 5 10	1044 1019 999	Area
10	160 240 320	0·8	2	118	5	1234 1337 1418	E.A.S.
10	240	0·4 0·6 0·8	2	118	5	1541 1419 1337	Emissivity
10	240	0·8	1 2 5	118	5	1348 1337 1334	Radius
10	240	0·8	2	24 59 118	2·5 5 5	1527 1409 1337	Conductivity
10	240	0·8	2	118	2·5 5 10	1369 1337 1314	Area

Some results appear in the Table more than once to make comparison easier.

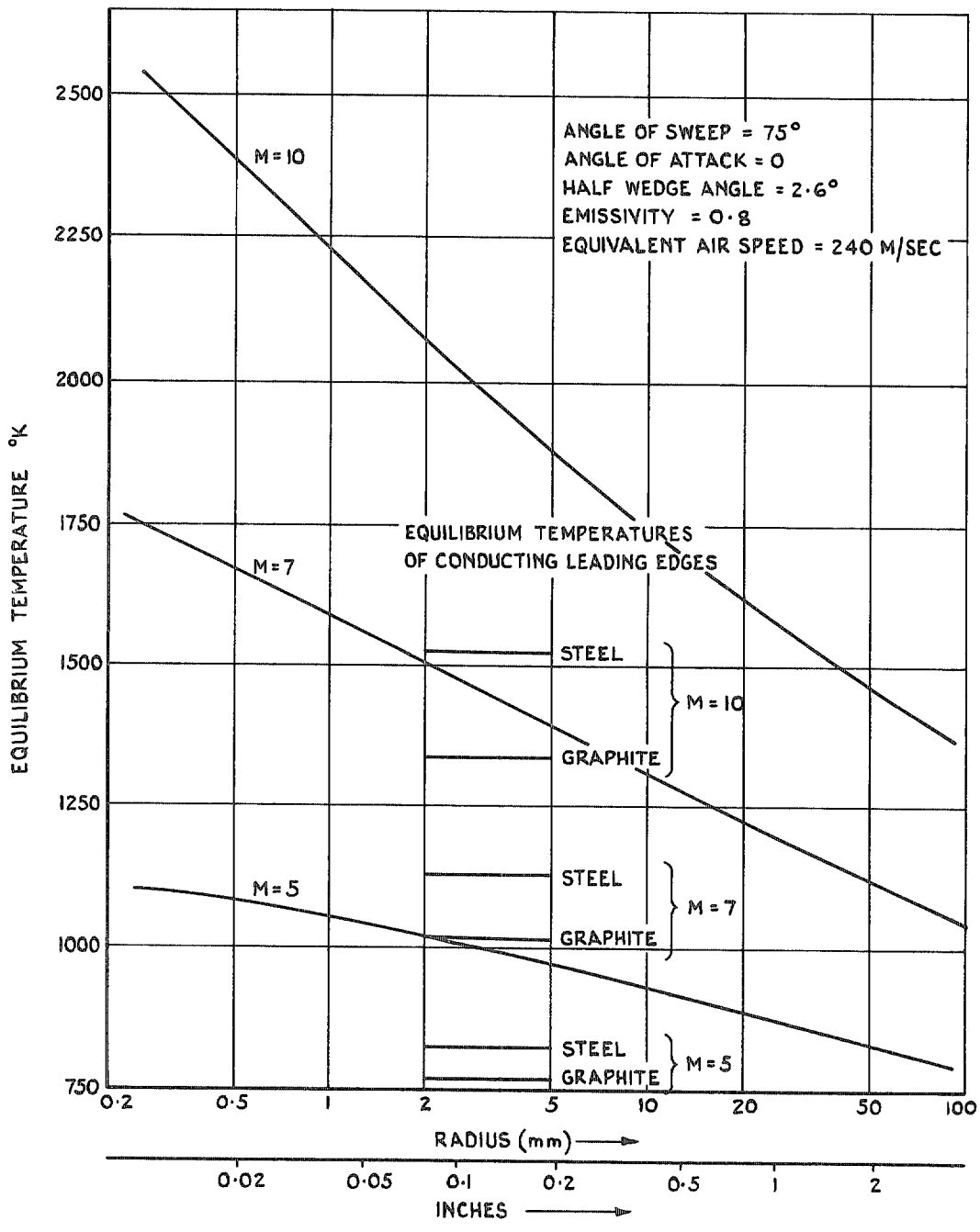

FIG. 7. Variation of stagnation-line equilibrium temperature with leading-edge radius.

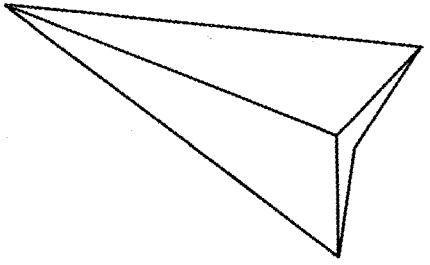

FIG. 1a. Perspective.

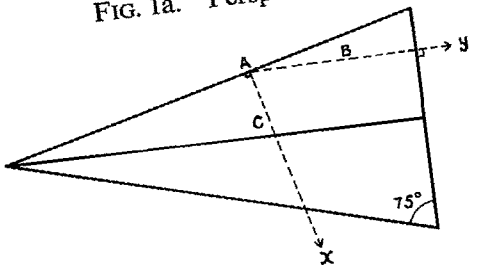

FIG. 1b. Plan.

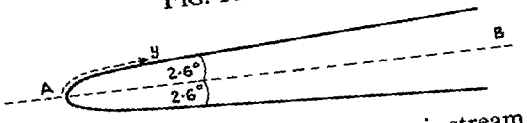

FIG. 1c. Vertical plane parallel to air stream.

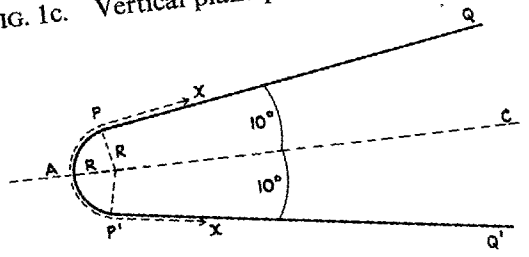

FIG. 1d. Vertical plane perpendicular to leading edge.

FIG. 1. Sections of wing.

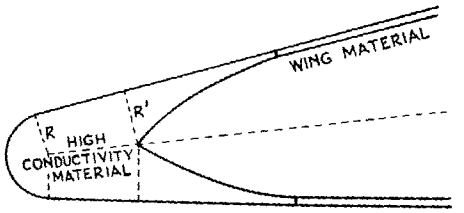

FIG. 2a. High conductivity leading edge.

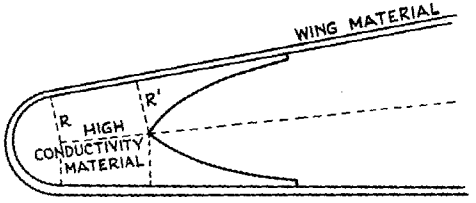

FIG. 2b. Leading edge with insert of high conductivity material.

FIG. 2. Conducting leading edges.

Sections perpendicular to leading edge

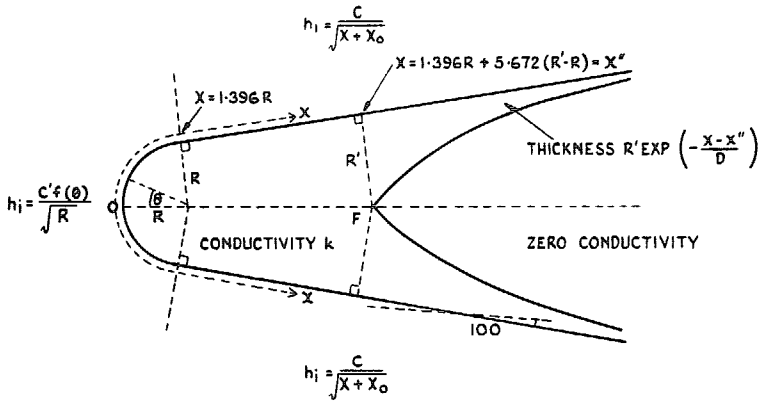

FIG. 3a. Heat transfer; distribution of material.

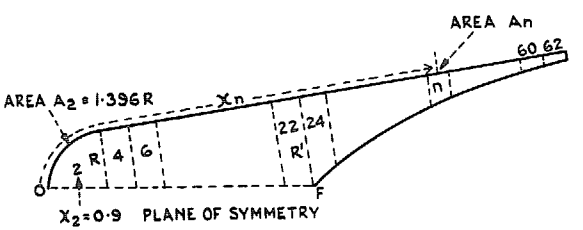

FIG. 3b. Segmentation of conducting material.

FIG. 3. Leading edge showing heat-transfer coefficients and distribution and segmentation of conducting material.

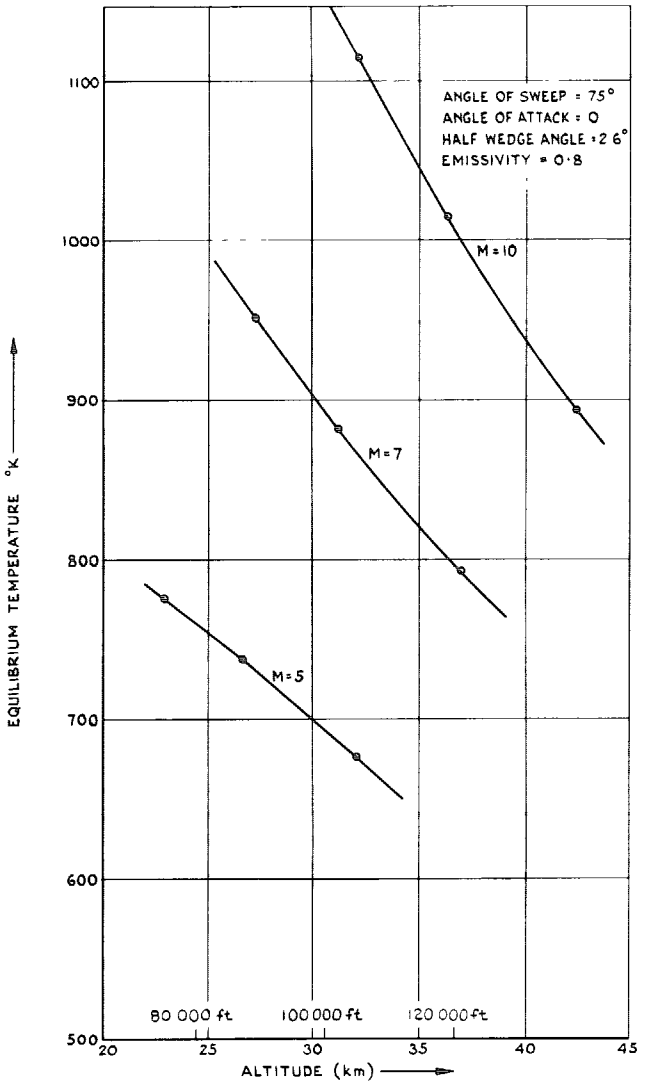

FIG. 4. Equilibrium temperatures with turbulent flow 15 metres (50 ft) from onset of turbulence.

Dd.129527 K.5 Printed in Wales for Her Majesty's Stationery Office by Allens Printers (Wales) Limited

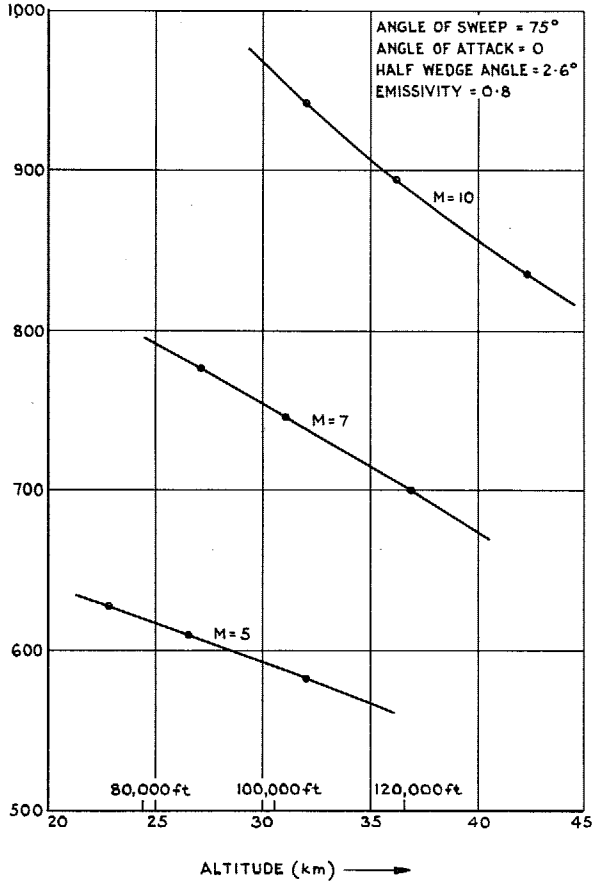

FIG. 5. Equilibrium temperatures with laminar flow 0·915 metres (3 ft) from sharp leading edge.

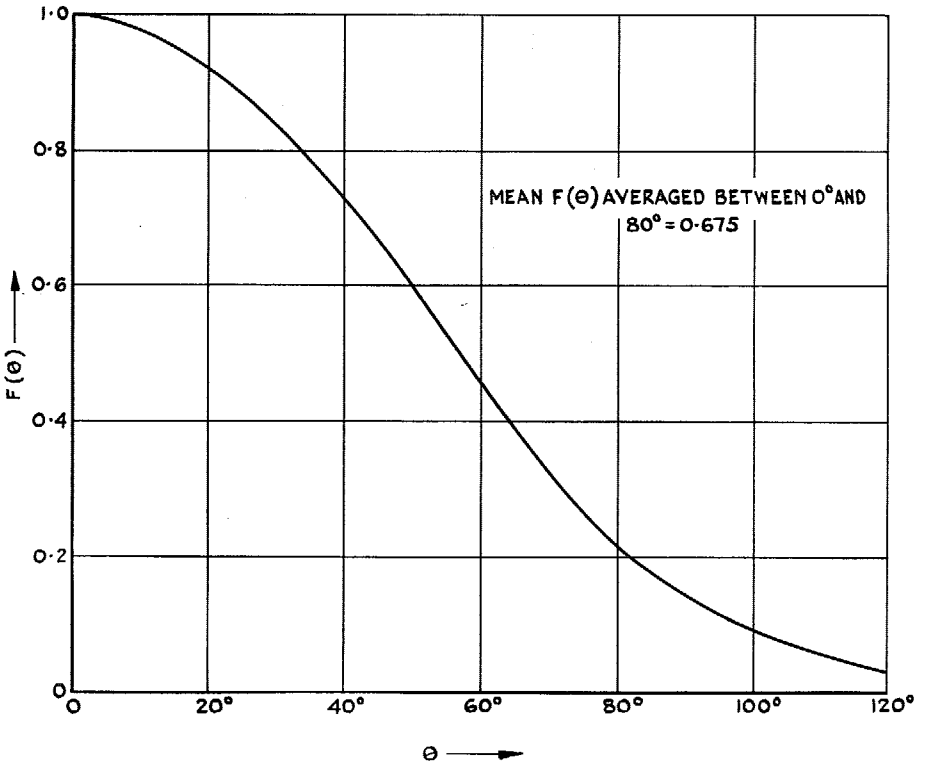

FIG. 6. Variation of heat-transfer coefficient with angular distance from stagnation line.

Published by
HER MAJESTY'S STATIONERY OFFICE

To be purchased from
49 High Holborn, London W.C.1
423 Oxford Street, London W.1
13A Castle Street, Edinburgh 2
109 St. Mary Street, Cardiff CF1 1JW
Brazennose Street, Manchester 2
50 Fairfax Street, Bristol 1
258–259 Broad Street, Birmingham 1
7–11 Linenhall Street, Belfast BT2 8AY
or through any bookseller

S.O. Code No. 23-3540